Surface gravity waves over a two-dimensional random seabed

Jørgen H. Pihl,* Chiang C. Mei,† and Matthew J. Hancock‡
Department of Civil and Environmental Engineering, Massachusetts Institute of Technology, Cambridge, Massachusetts 02139
(Received 20 January 2002; published 26 July 2002)

We extend homogenization theory to study the two-dimensional evolution of weakly nonlinear waves in a sea where the bathymetry is random over a large area. A deterministic nonlinear Schrödinger equation is derived for the envelope of a nearly sinusoidal progressive wave train. Randomness is shown to yield a linear term with a complex coefficient depending on a certain statistical average of the bathymetry. Numerical solutions are discussed for the diffraction of a Stokes wave in head-sea incidence towards a bathymetry of given plan form. Effects of the height and plan form of the randomness, as well as wave nonlinearity are examined analytically and numerically.

DOI: 10.1103/PhysRevE.66.016611 PACS number(s): 05.45.Yv, 46.65.+g, 47.35.+i, 47.45.−n

I. INTRODUCTION

There is a rich literature on the propagation of infinitesimal waves in randomly disordered media. The techniques of analysis range from perturbation approximations [1–6] to Feynman diagrams [7–10] to analytical theories combined with numerical computations [11–13]. An important physical consequence is Anderson localization [14], in which disorder leads to exponential attenuation in space for nearly all frequencies, in contrast to periodic media where Bragg scattering is effective only within certain frequency-bands.

In recent years many theories on nonlinear waves in random media have also appeared. Devillard and Souillard [15] have studied the one-dimensional nonlinear Schrödinger equation with a random potential. For a slab of randomness of thickness L, they found that the transmitted wave diminishes exponentially with increasing L if nonlinearity is weak. For strong nonlinearity, the attenuation is only polynomial. Extensions of this work for incident solitons and other types of random potentials have been advanced by many researchers (e.g., Refs. [16–20]). For extensive reviews, see Refs. [21,22]. A theory for the Korteweg–de Vries (KdV) equation with a weak random potential has also been studied in Ref. [23]. In these mathematical models, a common feature is that the final differential equation has one or more stochastic coefficients.

Suggested by the perturbation theories of Keller and Karal [3,4] on one-dimensional infinitesimal waves, we have recently used the method of multiple scales to examine the spatial attenuation of weakly nonlinear and dispersive waves by random irregularities [24]. The standard technique of homogenization, well known for periodic media, was found to be effective for a weakly nonlinear string embedded in an elastic surrounding with a weakly random elasticity. The envelope of unidirectional narrow-banded waves is found to be governed by a nonlinear Schrödinger equation with a *deterministic* potential amounting to damping, with the complex damping coefficient being the statistical average of the random perturbations. Steady nonlinear waves were found analytically to suffer exponential attenuation (localization). By numerical means, transient waves were also studied.

In coastal oceanography, the propagation of sea waves over an irregular seabed is of practical interest. A few theoretical works on weakly nonlinear sea waves have been advanced by using diagrammatic methods [25,26] or perturbation analysis [27,28]. Recently, we have extended the homogenization theory to the one-dimensional propagation of slowly modulated, unidirectional water waves over a weakly random seabed [29]. In this paper, we make a further extension to a random sea bed of two-dimensional plan form. A spatially two-dimensional nonlinear Schrödinger equation is derived for the wave envelope, where a deterministic potential arises whose complex coefficient is a certain average involving the random bathymetry. Analytical formulas of the coefficient are obtained. Moreover, the forward propagation and diffraction of uniform incident waves by an area of random seabed is studied numerically, to examine the physical effects of the mean-square height and overall geometry of the random area, as well as nonlinearity.

II. THE WAVE ENVELOPE EQUATION

The derivation here is a direct extension of the known approach for the classical case of a horizontal seabed. As usual, the three-dimensional fluid motion is assumed to be inviscid and irrotational. The governing Laplace equation and nonlinear boundary conditions for the velocity potential $\phi(\vec{x},z,t)$ and the free surface displacement $\eta(\vec{x},t)$ are well known (e.g., Ref. [30]). Focusing attention on gently sloping waves and bathymetric irregularities, we define the small parameter ε as the typical slope of both the free surface and the seabed roughness, i.e., $k\eta \sim kb = O(\varepsilon) \ll 1$. On the seabed $z=-h+\varepsilon b(\vec{x})$, where the mean depth h is constant, but $b(\vec{x})$ is a random function of $\vec{x}$ with zero mean; the normal velocity must vanish,

$$\phi_z - \varepsilon \nabla b \cdot \nabla \phi = 0, \quad z=-h+\varepsilon b. \tag{1}$$

Taylor expansions about the mean allow us to apply the sea surface conditions along $z=0$ and the bottom condition

*Present address: Øverødvej 23, 1-12, DAK-2840 Holt, Denmark. Electronic address: jh@pihl.as
†Electronic address: ccmei@mit.edu
‡Electronic address: hancock@mit.edu

along $z=-h$. To allow for slow modulations due to narrow bandwidth of frequencies, weak nonlinearity and slow spatial attenuation, we introduce the multiple scale variables $\vec{x}_1=\varepsilon\vec{x}$, $\vec{x}_2=\varepsilon^2\vec{x},\ldots$ and $t_1=\varepsilon t$, $t_2=\varepsilon^2 t,\ldots$.

We also assume that the correlation length of the random depth perturbations is of the order of the typical wavelength. From linearized theories, it is known that the length scale of attenuation due to random scattering is of the order $O(1/k\varepsilon^2)$. In order that such effects are significant, we assume that b is characterized by two scales, one for the local fluctuations and one for the global extent of the random region, i.e., $b=b(\vec{x},\vec{x}_2)$.

After introducing the perturbation expansions for the velocity potential ϕ and free surface height η,

$$\phi=\phi_1+\varepsilon\phi_2+\varepsilon^2\phi_3+\ldots, \tag{2}$$

$$\eta=\eta_1+\varepsilon\eta_2+\varepsilon^2\eta_3+\ldots, \tag{3}$$

a set of perturbation equations for ascending orders in ε is obtained, which are similar to those for the simpler case of a horizontal seabed [30]. We follow Eq. (29) for the two-dimensional problem (x,z) with a one-dimensional bathymetry $b(x,x_2)$, and separate the unknown potential and surface height of the nth order in two parts, the mean and the random fluctuation from the mean,

$$\phi_n=\langle\phi_n\rangle+\phi_n', \quad \eta_n=\langle\eta_n\rangle+\eta_n'. \tag{4}$$

Similar separation of the perturbation equations at each order yields a set of boundary value problems for the mean and for the random fluctuations. At the leading order $O(\varepsilon^0)$ there is no random part; the mean is taken to be a train of plane progressive waves of amplitude A over a horizontal bottom, governed by homogeneous equations. Information on the evolution of A is found by examining the solvability of the inhomogeneous problems for the mean at higher orders and by solving the problems for the random fluctuations.

Specifically, from the Laplace equation, we obtain at order n,

$$\left(\boldsymbol{\nabla}^2+\frac{\partial^2}{\partial z^2}\right)\phi_n=F_n, \quad -h<z<0. \tag{5}$$

On the mean sea surface, we have

$$\mathcal{L}\phi_n\equiv\left(g\frac{\partial}{\partial z}+\frac{\partial^2}{\partial t^2}\right)\phi_n=G_n, \quad z=0, \tag{6}$$

which incorporates both kinematic and dynamic requirements. The nth order seabed condition is

$$\frac{\partial\phi_n}{\partial z}=I_n, \quad z=-h. \tag{7}$$

Once the velocity potential is found, the free surface height follows from the dynamic condition (the Bernoulli equation) of zero pressure,

$$-g\eta_n=\phi_{nt}+H_n, \quad z=0, \tag{8}$$

where we denote partial derivatives with respect to t and z by subscripts. All forcing terms F_n, G_n, H_n, and I_n are expressible in terms of the lower order solutions $\phi_{n-1},\ldots,\phi_1$.

At the leading order, the forcing terms for the boundary value problem of ϕ_1 are all zero, i.e., $F_1=G_1=I_1=H_1=0$. Formally, randomness has yet no direct effects, so that ϕ_1 and η_1 are equal to their statistical averages, denoted by $\langle\phi_1\rangle$ and $\langle\eta_1\rangle$, respectively. The random components, denoted by primes, vanish:

$$\phi_1'=\eta_1'=0. \tag{9}$$

We take the homogeneous solution to be a monochromatic wave train propagating in the direction of x from left to right,

$$\eta_1=\langle\eta_1\rangle=\frac{A}{2}e^{i\psi}+\text{c.c.}=\text{Re}\{Ae^{i\psi}\} \tag{10}$$

and

$$\begin{aligned}\phi_1=\langle\phi_1\rangle&=\phi_{10}+(\phi_{11}e^{i\psi}+\text{c.c.})\\&=\phi_{10}-\frac{g}{2\omega}\frac{\cosh[k(z+h)]}{\cosh(kh)}(iAe^{i\psi}+\text{c.c.})\end{aligned} \tag{11}$$

(see, e.g., Ref. [30]). Here, $A(\vec{x}_1,\vec{x}_2;t_1,t_2)$ denotes the leading-order wave amplitude and $\psi=\vec{k}\cdot\vec{x}-\omega t=kx-\omega t$ is the wave phase [31]. The zeroth harmonic $\phi_{10}=\phi_{10}(\vec{x}_1,\vec{x}_2,t_1,t_2,\ldots)$ represents the long-wave potential. The angular frequency ω is related to the wave number k via the dispersion relation

$$\omega^2=gk\tanh(kh). \tag{12}$$

At the second order $O(\varepsilon)$, the forcing terms are:

$$F_2=-2\boldsymbol{\nabla}\cdot\boldsymbol{\nabla}_1\phi_1,$$

$$G_2=-\{\eta_1\mathcal{L}_z\phi_1+[(\boldsymbol{\nabla}\phi_1)^2+\phi_{1z}^2]_t+2\phi_{1tt_1}\},$$

where the linear operator $\mathcal{L}$ is defined in Eq. (6) and

$$I_2=\boldsymbol{\nabla}\cdot(b\boldsymbol{\nabla}\phi_1), \tag{13}$$

which is a random function of $\vec{x}$ and $\vec{x}_2$. In addition, from the Bernoulli equation, we have

$$H_2=\frac{1}{2}[(\boldsymbol{\nabla}\phi_1)^2+\phi_{1z}^2]+\phi_{1t_1}+\eta_1\phi_{1zt}.$$

Again, the potential ϕ_2 and the forcing functions F_2 and G_2 can be expressed as the sum of statistical averages and random fluctuations. Because $\langle b\rangle=0$, we find that $\langle F_2\rangle=F_2$, $\langle G_2\rangle=G_2$, $\langle H_2\rangle=H_2$, and $\langle I_2\rangle=0$. Thus, the randomness does not affect the mean components at order $O(\varepsilon)$. Solvability of the first harmonic $\langle\phi_{21}\rangle$ gives the well-known law of wave action conservation

$$\frac{\partial A}{\partial t_1}+c_g\frac{\partial A}{\partial x_1}=0, \tag{14}$$

where

$$c_g=\frac{\partial \omega}{\partial k}=\frac{\omega}{2k}\left(1+\frac{2kh}{\sinh(2kh)}\right) \tag{15}$$

is the group velocity.

The random component is caused by the interaction of the incident plane wave and the random perturbations on the seabed,

$$\frac{\partial \phi_2'}{\partial z}=I_2'=\nabla\cdot(b\nabla\phi_1), \quad z=-h.$$

Hence, ϕ_2' contains only the first time harmonic,

$$\phi_2'=\phi_{21}'e^{-i\omega t}+\text{c.c.}, \quad \eta_2'=\eta_{21}'e^{-i\omega t}+\text{c.c.} \tag{16}$$

The boundary-value problem for ϕ_{21}' is governed by

$$\left(\frac{\partial^2}{\partial z^2}+\nabla^2\right)\phi_{21}'=0, \quad -h<z<0,$$

$$\left(g\frac{\partial}{\partial z}-\omega^2\right)\phi_{21}'=0, \quad z=0,$$

$$\frac{\partial \phi_{21}'}{\partial z}=\nabla\cdot[b\nabla(\phi_{11}e^{i\vec{k}\cdot\vec{x}})]$$

$$=\frac{g\vec{k}A}{2\omega\cosh(kh)}\cdot\nabla[b(\vec{x})e^{i\vec{k}\cdot\vec{x}}], \quad z=-h.$$

To solve for ϕ_{21}', we define Green's function $\mathcal{G}(\vec{x},z;\vec{x}')$ by

$$\nabla^2\mathcal{G}+\mathcal{G}_{zz}=0, \quad -h<z<0, \tag{17}$$

$$\mathcal{G}_z-\frac{\omega^2}{g}\mathcal{G}=0, \quad z=0, \tag{18}$$

$$\mathcal{G}_z=\delta(\vec{x}-\vec{x}'), \quad z=-h. \tag{19}$$

In addition, $\mathcal{G}$ is required to behave as an outgoing wave at infinity. The solution for ϕ_{21}' is found by using Green's theorem,

$$\phi_{21}'=\frac{gA}{2\omega\cosh(kh)}\int \vec{k}\cdot\nabla'[b(\vec{x}')e^{i\vec{k}\cdot\vec{x}'}]\mathcal{G}(|\vec{\xi}|,z)d\vec{x}', \tag{20}$$

where, for brevity, $\vec{\xi}\equiv\vec{x}-\vec{x}'$. The Green's function is shown below, while the derivation is outlined in the Appendix,

$$\mathcal{G}(|\vec{x}-\vec{x}'|,z)=-i\frac{\frac{\omega^2}{2g}H_0^{(1)}(k|\vec{\xi}|)}{\frac{\omega^2h}{g}+\sinh^2(kh)}\cosh[k(z+h)]$$
$$-\frac{1}{\pi}\sum_n\frac{\frac{\omega^2}{g}K_0(k_n|\vec{\xi}|)}{\frac{\omega^2h}{g}-\sin^2(k_nh)}\cos[k_n(z+h)], \tag{21}$$

where $H_0^{(1)}=J_0+iY_0$ denotes the Hankel function of the first kind and K_0 is the modified Bessel function.

At the third order $O(\varepsilon^2)$, only the equations for the statistical average $\langle\phi_3\rangle$ are needed:

$$\left(\nabla^2+\frac{\partial^2}{\partial z^2}\right)\langle\phi_3\rangle=\langle F_3\rangle, \quad -h<z<0, \tag{22}$$

$$\mathcal{L}\langle\phi_3\rangle=\langle G_3\rangle, \quad z=0, \tag{23}$$

$$\frac{\partial\langle\phi_3\rangle}{\partial z}=\langle I_3\rangle, \quad z=-h, \tag{24}$$

where the operator $\mathcal{L}$ is defined in Eq. (6). Using the fact that ϕ_1 and η_1 are deterministic, the forcing functions at $O(\varepsilon^2)$ can be simplified to

$$\langle F_3\rangle=-[\nabla_1^2\phi_1+2\nabla\cdot\nabla_2\phi_1+2\nabla\cdot\nabla_1\langle\phi_2\rangle],$$

$$\begin{aligned}\langle G_3\rangle=-\Big[&\langle\eta_2\rangle\mathcal{L}_z\phi_1+\eta_1\mathcal{L}_z\langle\phi_2\rangle+\frac{1}{2}\eta_1^2\mathcal{L}_{zz}\phi_1\\&+2(\nabla\phi_1\cdot\nabla\langle\phi_2\rangle+\phi_{1z}\langle\phi_2\rangle_z)_t+\eta_1[(\nabla\phi_1)^2+\phi_{1z}^2]_{tz}\\&+\frac{1}{2}\left(\nabla\phi_1\cdot\nabla+\phi_{1z}\frac{\partial}{\partial z}\right)[(\nabla\phi_1)^2+\phi_{1z}^2]+2\langle\phi_2\rangle_{tt_1}\\&+2\phi_{1z}\phi_{1zt_1}+2\nabla_1\phi_1\cdot\nabla\phi_{1t}+2\nabla\phi_1\cdot\nabla\phi_{1t_1}\\&+2\nabla\phi_1\cdot\nabla_1\phi_{1t}+2\eta_1\phi_{1ztt_1}+2\phi_{1tt_2}+\phi_{1t_1t_1}\Big].\end{aligned}$$

Since ϕ_1, $\langle\eta_2\rangle$, and $\langle\phi_2\rangle$ are independent of $b(\vec{x},\vec{x}_2)$, $\langle F_3\rangle$, and $\langle G_3\rangle$ are formally identical to those for a horizontal seabed [30]. The bed roughness $b(\vec{x},\vec{x}_2)$ only affects $\langle I_3\rangle$. From Eq. (13), we have, on the mean seabed $z=-h$,

$$\begin{aligned}\langle I_3\rangle&=\langle\nabla\cdot(b\nabla\phi_2)\rangle|_{z=-h}=\langle\nabla\cdot[b(\nabla\langle\phi_2\rangle+\nabla\phi_2')]\rangle|_{z=-h}\\&=\langle\nabla\cdot(b\nabla\phi_2')\rangle|_{z=-h}.\end{aligned} \tag{25}$$

In view of Eq. (20), the right-hand side above contains only the first harmonic and can be written in the form

$$\langle I_3\rangle=i\beta\cosh(kh)Ae^{i\psi}+\text{c.c.}, \tag{26}$$

where $\beta(\vec{x}_2)$ is a complex coefficient that is discussed in the following section.

We now separate $<\phi_3>$ into different harmonics:

$$\langle\phi_3\rangle=\langle\phi_{30}\rangle+(\langle\phi_{31}\rangle e^{i\psi}+\text{c.c.})+\cdots$$
$$=\langle\phi_{30}\rangle+(e^{i\psi}F(\vec{x}_2,z,t_2)+\text{c.c.})+\cdots, \tag{27}$$

where randomness only affects the first harmonic in view of Eq. (26). In particular, $\langle\phi_{30}\rangle$ is governed by equations unaffected by the bathymetry, and hence the solvability condition for $\langle\phi_{30}\rangle$ is formally the same as that for a horizontal seabed [Ref. [30], Eq. (2.36), p. 613]:

$$\frac{\partial^2\phi_{10}}{\partial t_1^2}-gh\left(\frac{\partial^2\phi_{10}}{\partial x_1^2}+\frac{\partial^2\phi_{10}}{\partial y_1^2}\right)=\frac{\omega^3\cosh^2(kh)}{2k\sinh^2(kh)}\frac{\partial|A|^2}{\partial x_1}-\frac{\omega^2}{4\sinh^2(kh)}\frac{\partial|A|^2}{\partial t_1}. \tag{28}$$

Thus, long waves are forced by the slow modulation of the short-wave envelope. As for the first harmonic in $<\phi_3>$, we substitute Eqs. (26) and (27) into Eqs. (22)–(24), to obtain the inhomogeneous boundary-value problem,

$$\frac{\partial^2F}{\partial z^2}-k^2F=F_{31},\quad -h<z<0,$$

$$\frac{\partial F}{\partial z}-\frac{\omega^2}{g}F=\frac{1}{g}G_{31},\quad z=0,$$

$$\frac{\partial F}{\partial z}=i\beta A\cosh(kh),\quad z=-h,$$

where $\langle F_{31}\rangle,\langle G_{31}\rangle$ are the complex first harmonic amplitudes of $[F_3]$ and $[G_3]$, and are given in Ref. [30] [Eqs. (2.37) and (2.38), p. 613]. Since the inhomogeneous boundary-value problem above has a nontrivial homogeneous solution ϕ_{11}, we invoke the solvability condition to obtain

$$\left(\frac{\partial}{\partial t_2}+c_g\frac{\partial}{\partial x_2}\right)A+i\left\{-\frac{\omega''}{2}\frac{\partial^2A}{\partial x_1^2}-\frac{c_g}{2k}\frac{\partial^2A}{\partial y_1^2}+\alpha_1|A|^2A-\alpha_2A-\beta A\right\}=0. \tag{29}$$

The coefficients are

$$\omega''=\frac{\partial^2\omega}{\partial k^2}=\frac{c_g^2}{\omega}-\frac{\omega}{2k^2}\left(1+\frac{2kh\cosh(2kh)}{\sinh(2kh)}\right),$$

$$\alpha_1=\frac{\omega k^2[\cosh(4kh)+8-2\tanh^2(kh)]}{16\sinh^4(kh)},$$

and

$$\alpha_2=\frac{k^2}{2\omega\cosh^2(kh)}\frac{\partial\phi_{10}}{\partial t_1}-k\frac{\partial\phi_{10}}{\partial x_1}.$$

The factor $2\alpha_1/k^3c_g=\Theta$ can be found in Ref. [30] (Fig. 8.2, p. 654).

Finally, combining Eqs. (14) and (29) yields

$$\left(\frac{\partial}{\partial t_1}+c_g\frac{\partial}{\partial x_1}\right)A+i\varepsilon\left\{-\frac{\omega''}{2}\frac{\partial^2A}{\partial x_1^2}-\frac{c_g}{2k}\frac{\partial^2A}{\partial y_1^2}+\alpha_1|A|^2A-\alpha_2A-\beta A\right\}=0. \tag{30}$$

This is a nonlinear two-dimensional Schrödinger equation modified by the linear term with the complex and deterministic coefficient $\beta=\beta_r+i\beta_i$, which represents the effects of the random bathymetry. Before studying its properties, we need to evaluate this coefficient.

III. THE COEFFICIENT β

Inserting Eqs. (20) into (16) yields

$$\phi_2'=\frac{gAe^{-i\omega t}}{2\omega\cosh(kh)}\int\vec{k}\cdot\nabla'[b(\vec{x}')e^{i\vec{k}\cdot\vec{x}'}]\mathcal{G}(|\vec{x}-\vec{x}'|,z)d\vec{x}'+\text{c.c.}, \tag{31}$$

whose gradient can be straightforwardly calculated. From Eqs. (25) and (31), we obtain, after some algebra,

$$\frac{\langle I_3\rangle}{\cosh(kh)}=\frac{\nabla\cdot\langle b\nabla\phi_2'\rangle|_{z=-h}}{\cosh(kh)}$$
$$=-\frac{igAe^{i(kx-\omega t)}}{2\omega\cosh^2(kh)}\int\vec{k}\cdot\nabla^{\xi}[C(\vec{\xi})e^{-i\vec{k}\cdot\vec{\xi}}]\times(\vec{k}\cdot\nabla^{\xi}|\vec{\xi}|)\mathcal{G}'(|\vec{\xi}|,-h)d\vec{\xi}+\text{c.c.}, \tag{32}$$

where $\vec{\xi}=\vec{x}-\vec{x}'$; $\mathcal{G}'(|\vec{\xi}|,-h)$ denotes the derivative with respect to the scalar $\xi=|\vec{\xi}|$, ∇^{ξ} denotes the gradient operator with respect to ξ, and $C(\vec{\xi})=\langle b(\vec{x})b(\vec{x}')\rangle$ is the two-point covariance function that may also depend on the slow coordinate $\vec{x}_2$. This dependence will not be displayed for brevity.

Note that

$$\vec{k}\cdot\nabla^{\xi}|\vec{\xi}|=\vec{k}\cdot\frac{\vec{\xi}}{\xi}=k\cos\theta, \tag{33}$$

where θ is the angle of $\vec{\xi}$ relative to $\vec{k}$ that is along the positive x axis. Thus, from Eqs. (26), (32), and (33), we obtain

$$\beta=-\frac{gk}{2\omega\cosh^2(kh)}\times\int\vec{k}\cdot\nabla^{\xi}[C(\vec{\xi})e^{-i\vec{k}\cdot\vec{\xi}}]\cos(\theta)\mathcal{G}'(|\vec{\xi}|,-h)d\vec{\xi}=\frac{k^2c_g\left(\tau_0+\sum_n\tau_n\frac{\frac{\omega^2h}{g}+\sinh^2(kh)}{\frac{\omega^2h}{g}-\sin^2(k_nh)}\right)}{2[kh+\sinh(kh)\cosh(kh)]^2},\tag{34}$$

where

$$\tau_0=-k\int\vec{k}\cdot\nabla^{\xi}[C(\vec{\xi})e^{-i\vec{k}\cdot\vec{\xi}}]\cos(\theta)H_1^{(1)}(k|\vec{\xi}|)d\vec{\xi}\tag{35}$$

and

$$\tau_n=-\frac{2}{\pi}k_n\int\vec{k}\cdot\nabla^{\xi}[C(\vec{\xi})e^{-i\vec{k}\cdot\vec{\xi}}]\cos(\theta)K_1(k_n|\vec{\xi}|)d\vec{\xi}.\tag{36}$$

For two-dimensional random media, the isotropic model is commonly used for simplicity. Its covariance C depends only on the distance between two points, i.e., $C=C(\xi)$. It follows that

$$\nabla[C(\xi)e^{-i\vec{k}\cdot\vec{\xi}}]=[(\nabla|\vec{\xi}|)C'(\xi)-i\vec{k}C(\xi)]e^{-i\vec{k}\cdot\vec{\xi}}.$$

Inserting this and Eqs. (33) into (35) and using polar coordinates yields

$$\begin{aligned}\mathrm{Im}\{\tau_0\}&=-k^2\int_0^{\infty}\int_{-\pi}^{\pi}[\cos^2(\theta)C'(\xi)\\&\quad-ik\cos\theta C(\xi)]e^{-ik\xi\cos\theta}J_1(k\xi)\xi d\theta d\xi\\&=-\pi k^2\int_0^{\infty}\xi C'(\xi)J_1(k\xi)\frac{1}{2\pi}\\&\quad\times\int_{-\pi}^{\pi}(1-\cos 2\theta)e^{-ik\xi\cos\theta}d\theta d\xi-2\pi k^3\\&\quad\times\int_0^{\infty}\xi C(\xi)J_1(k\xi)\frac{(-i)}{2\pi}\\&\quad\times\int_{-\pi}^{\pi}\cos\theta e^{-ik\xi\cos\theta}d\theta d\xi.\end{aligned}$$

Since

$$J_n(k|\vec{\xi}|)=\frac{(-i)^n}{2\pi}\int_{-\pi}^{\pi}e^{ik|\vec{\xi}|\cos\theta}\cos(n\theta)d\theta,$$

we further obtain

$$\mathrm{Im}\{\tau_0\}=-\pi k^2\int_0^{\infty}\xi C'(\xi)J_1(k\xi)[J_0(k\xi)-J_2(k\xi)]d\xi+2\pi k^3\int_0^{\infty}\xi C(\xi)J_1^2(k\xi)d\xi.\tag{37}$$

Similarly, the real parts of Eqs. (35) and (36) can be simplified to

$$\mathrm{Re}\{\tau_0\}=\pi k^2\int_0^{\infty}\xi C'(\xi)Y_1(k\xi)[J_0(k\xi)-J_2(k\xi)]d\xi-2\pi k^3\int_0^{\infty}\xi C(\xi)Y_1(k\xi)J_1(k\xi)d\xi\tag{38}$$

and

$$\tau_n=-2kk_n\int_0^{\infty}\xi C'(\xi)K_1(k_n\xi)[J_0(k\xi)-J_2(k\xi)]d\xi+4k^2k_n\int_0^{\infty}\xi C(\xi)K_1(k_n\xi)J_1(k\xi)d\xi,\tag{39}$$

which is real.

For explicit results, we consider the Gaussian covariance

$$C(\xi)=\sigma^2(\vec{x}_2)e^{-\alpha^2\xi^2},\tag{40}$$

where $\sigma(\vec{x}_2)$ is the root mean square height of random perturbations and α is the reciprocal of the correlation length. Substituting Eq. (40) and the dimensionless variables $R=\alpha\xi$, $\kappa=k/\alpha$, and $\kappa_n=k_n/\alpha$ into Eqs. (37), (38), and (39) yields

$$\frac{\mathrm{Im}\{\tau_0\}}{k\sigma^2}=2\pi\kappa\int_0^{\infty}Re^{-R^2}J_1(\kappa R)[RJ_0(\kappa R)-RJ_2(\kappa R)+\kappa J_1(\kappa R)]dR,\tag{41}$$

$$\frac{\mathrm{Re}\{\tau_0\}}{k\sigma^2}=-2\pi\kappa\int_0^{\infty}Re^{-R^2}Y_1(\kappa R)[RJ_0(\kappa R)-RJ_2(\kappa R)+\kappa J_1(\kappa R)]dR,\tag{42}$$

and

$$\frac{\tau_n}{k\sigma^2}=4\kappa_n\int_0^{\infty}Re^{-R^2}K_1(\kappa_nR)[RJ_0(\kappa R)-RJ_2(\kappa R)+\kappa J_1(\kappa R)]dR.\tag{43}$$

The right-hand sides of Eqs. (41), (42), and (43) are just functions of $\kappa=k/\alpha$ and kh. A similar result has been obtained in Ref. [29] for a one-dimensional bathymetry, where the depth contours are parallel,

$$\frac{\tau_0}{k\sigma^2}=4+\pi\kappa e^{-\kappa^2}\mathrm{erfi}(\kappa)+i\sqrt{\pi}\kappa(1+e^{-\kappa^2}),\tag{44}$$

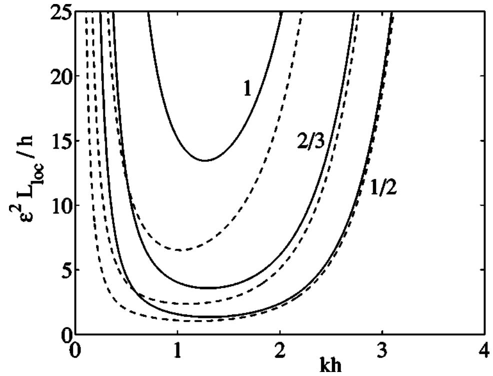

FIG. 1. Localization length to depth ratio $\varepsilon^2 L_{loc}/h$ corresponding to the 1D (broken) and 2D (solid) theories, for fixed roughness steepness $\alpha\sigma=1$ and various αh. Numbers adjacent to curves indicate the corresponding value of αh.

$$\frac{\tau_n}{k\sigma^2}=4-2\kappa_n\sqrt{\pi}\,\mathrm{Re}\left\{\exp\left(\frac{(\kappa_n+i\kappa)^2}{4}\right)\mathrm{erfc}\left(\frac{\kappa_n+i\kappa}{2}\right)\right\}, \tag{45}$$

where $\mathrm{erfi}(x)=i\,\mathrm{erf}(ix)$ is a real valued function of x.

Finally, we define the normalized β^* by

$$\beta^*=\frac{2\beta}{c_g k(k\sigma)^2}=\frac{\dfrac{\tau_0}{k\sigma^2}+\displaystyle\sum_n\frac{\tau_n}{k\sigma^2}\,\frac{\dfrac{\omega^2 h}{g}+\sinh^2(kh)}{\dfrac{\omega^2 h}{g}-\sin^2(k_n h)}}{[kh+\sinh(kh)\cosh(kh)]^2}, \tag{46}$$

which depends only on k/α and kh.

IV. A HALF PLANE OF RANDOMNESS

The main purpose of this paper is to examine the envelope evolution over a random seabed of two-dimensional plan form. For simplicity, we shall only consider a uniform Stokes wave arriving from $x\sim-\infty$, incident on a random bathymetry that is confined to the region $x>0$. Within this region of disorder, σ is taken to be a finite constant. As a preliminary, we recall first that a classical Stokes wave over a smooth seabed of constant depth has a uniform and stationary amplitude a and a phase that depends on a. If the region of randomness is infinite in width, i.e., $-\infty<y_1<\infty$, then Eq. (30) reduces to

$$ic_g A_{x_2}=-(\beta_r+i\beta_i)A+\alpha_1|A|^2A,\quad x_2>0.$$

The solution is a modified Stokes wave exponentially attenuated (localized) in the direction of propagation,

$$A=a_0e^{-\beta_i x_2/c_g}\exp\left(i\frac{\beta_r x_2}{c_g}+i\frac{\alpha_1 a_0^2}{2\beta_i}e^{-2\beta_i x_2/c_g}\right), \tag{47}$$

where a_0 is the amplitude at $x_2=0$, the border line of the region of randomness. From Eqs. (46) and (47), the dimensional localization distance is

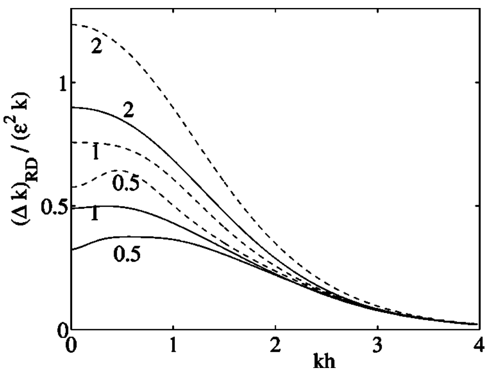

FIG. 2. $(\Delta k)_{RD}/(\varepsilon^2 k)$ as a function of kh with $\sigma/h=1$, for 1D (broken) and 2D (solid) theories. Numbers adjacent to curves indicate the corresponding value of αh.

$$L_{loc}=\frac{c_g}{\varepsilon^2\beta_i} \tag{48}$$

and is plotted in Fig. 1. Large σ (strong disorder) corresponds to large β_i and leads to fast attenuation. If the total length of the randomness is finite L, then the transmitted wave amplitude is obtained from Eq. (47) simply by replacing x_2 by L. The transmission coefficient decreases exponentially with L, implying localization. A similar result has been obtained in Ref. [29] for a one-dimensional bathymetry, where τ_0 and τ_n are given by Eqs. (44) and (45). From Fig. 1, the typical one-dimensional (1D) values for L_{loc} are somewhat smaller than the 2D values, implying that 1D randomness is a more effective damper. This is reasonable, as the flow can only pass 1D random undulations from above, whereas it also can circumvent 2D random undulations from the sides.

We remark that the exponential attenuation is independent of nonlinearity. This is in contrast with studies on the nonlinear Schrödinger equation with a random potential, where nonlinearity has the effect of delocalization, e.g., changing the spatial attenuation pattern from exponential to polynomial [15].

In view of Eqs. (10) and (47), we find that β contributes to an increase in wave number. The total increase is the sum of contributions from randomness and from nonlinearity,

$$\Delta k=(\Delta k)_{RD}+(\Delta k)_{NL}\equiv\frac{\varepsilon^2\beta_r}{c_g}-\frac{\varepsilon^2\alpha_1 a_0^2}{c_g}e^{-2\beta_i x_2/c_g}. \tag{49}$$

It is known that $\alpha_1>0$ (see Fig. 8.2, p. 654 in Ref. [30] where $\Theta=2\alpha_1/k^3c_g$ is plotted). Hence, increasing nonlinearity (εa_0) reduces the wave number and increases the wavelength, thereby increasing the group and phase speeds. This is a well-known result for Stokes waves. In this case, randomness also affects $(\Delta k)_{NL}$. Since the wave amplitude is attenuated by randomness, $(\Delta k)_{NL}$ diminishes with propagation distance. Randomness contributes more directly to the change in wave number via $(\Delta k)_{RD}$. As shown in Fig. 2, $(\Delta k)_{RD}$ is always positive, implying that the wavelength in the forward direction is shortened by random perturbations.

Since $\sigma/h=1$ is fixed, increasing αh is equivalent to increasing $\alpha\sigma$, implying steeper random roughness that is seen to shorten the waves. Also, 1D randomness has a stronger effect than 2D randomness, as is the case for the localization distance.

V. A WEDGE OF RANDOMNESS

Consider first a random region in the shape of a slender wedge or a triangle, whose vertex is at the origin. With $\partial A/\partial t_1=\partial A/\partial t_2=\partial A/\partial x_1=0$ but $\partial A/\partial y_1\neq 0$, Eq. (30) reduces to the damped nonlinear Schrödinger equation

$$ic_g A_{x_2}+\frac{c_g}{2k}A_{y_1y_1}=-(\beta_r+i\beta_i)A+\alpha_1|A|^2A. \tag{50}$$

Mathematically, the coordinate x_2 is timelike and y_1 is spacelike. In order to assess the effect of nonlinearity and randomness, we redefine the small parameter ε as the apex angle, so that the sides of the triangle are $y=\pm\varepsilon x$, $x>0$. Under the renormalization

$$B=A/A_0,\quad X=kx_2,\quad Y=ky_1, \tag{51}$$

the region of randomness is given by $Y<|X|$ and Eq. (50) becomes

$$2iB_X+B_{YY}=-\left(\frac{k\sigma}{\varepsilon}\right)^2\beta^*B+\left(\frac{kA_0}{\varepsilon}\right)^2\Theta|B|^2B. \tag{52}$$

β^* is finite and constant in the region of randomness $Y<|X|$ and zero outside, and

$$\Theta(kh)=\frac{\cosh(4kh)+8-2\tanh^2(kh)}{4\sinh^4(kh)\left(1+\dfrac{2kh}{\sinh(2kh)}\right)}>0,$$

which is positive and decreases monotonically with increasing kh (see Fig. 8.2, p. 654 in Ref. [30]). The parabolic equation (52) is solved by a finite difference numerical scheme [32].

Since $\Theta>0$, the nonlinear Schrödinger equation without the damping term is of defocusing type, and is stable to sideband disturbances if X and Y are regarded as time and space variables, respectively. To interpret certain numerical results later, we recall first the known analytical solution representing a dark (envelope-hole) soliton when $\beta=0$ (e.g., Ref. [33]),

$$B=b\,\frac{e^{2i\gamma}+e^{(kA_0/\varepsilon)\sqrt{2\Theta}b(Y-cX)\sin(\gamma)}}{1+e^{(kA_0/\varepsilon)\sqrt{2\Theta}b(Y-cX)\sin(\gamma)}}\,e^{-i/2[(kA_0)/\varepsilon]^2\Theta bX+i\alpha}. \tag{53}$$

The envelope has the largest depression along the axis $Y=cX$ and approaches asymptotically $be^{i\alpha}$ as $(Y-cX)\to\infty$. The parameter γ represents a phase change across the soliton hole so that the envelope towards $(Y-cX)\to-\infty$ is $be^{i(\alpha+2\gamma)}$. The slope c of the axis is related to b and γ by

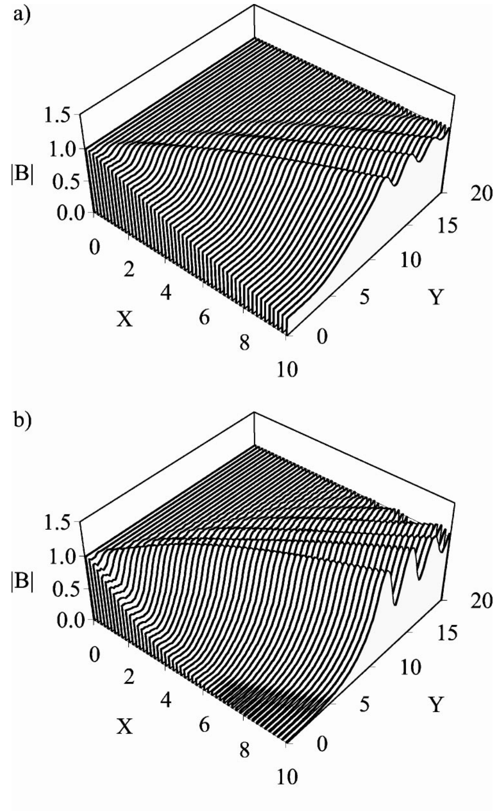

FIG. 3. Wave envelope over an infinite wedge-shaped region of randomness ($|Y|<X$) in the linear limit $kA_0/\varepsilon=0.0$, for different roughness heights (a) $k\sigma/\varepsilon=0.5$ and (b) $k\sigma/\varepsilon=1.0$.

$$c=\frac{kA_0}{\varepsilon}\sqrt{\frac{\Theta}{2}}\,b\cos(\gamma)=\pm\frac{kA_0}{\varepsilon}\sqrt{\frac{\Theta}{2}}\,(|B|_{min})^2, \tag{54}$$

where $(|B|_{min})^2=b^2\cos^2(\gamma)$ is the maximum depth of the envelope-hole along $Y=cX$.

We consider first the propagation of a Stokes wave train over a wedge-shaped region of randomness bounded by $Y=\pm X$. For both infinite $(0<X<\infty)$ and finite $(0<X<5)$ wedges, we plot the modulus of the envelope $|B|$ for $kh=0.7$, $k/\alpha=3$ (hence $\beta^*\approx 1.654+1.618i$), $kA_0/\varepsilon=0,0.5,1$ and $k\sigma/\varepsilon=0.5,1$, in order to examine the effects of randomness height and nonlinearity. Due to symmetry, only half of the wedge is shown for $Y>0$.

The case of an infinite wedge is shown in Figs. 3–5. For the linearized limit with $kA_0/\varepsilon=0$, the effect of increasing the roughness height is shown in Fig. 3. The height of the envelope is seen to decrease monotonically in the disordered region $Y<X$, as expected. Higher roughness accentuates the attenuation, so that waves are nearly absent in a centered wedge along $X>5$. Diffraction fringes are pronounced outside the wedge $Y>X$. With moderate nonlinearity (Fig. 4), the rate of attenuation is slightly reduced inside the wedge and diffraction is weakened outside. For the case of strong nonlinearity (Fig. 5), attenuation and diffraction are both further reduced, in qualitative agreement with existing theories for random potentials where disorder causes weaker localization.

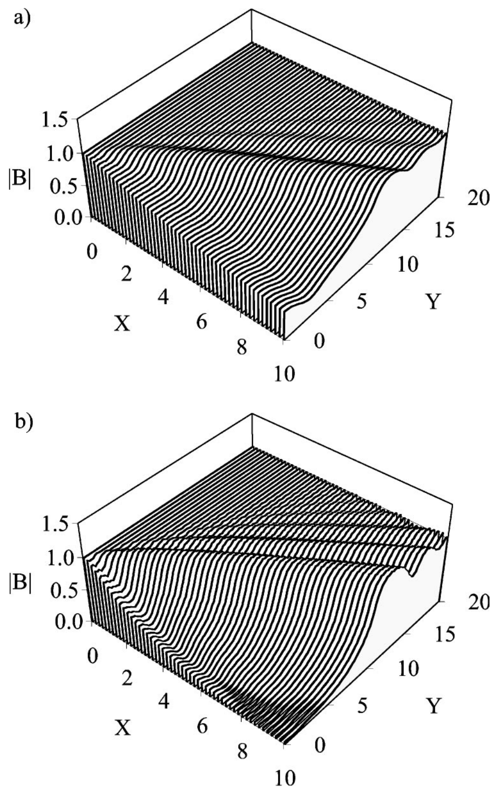

FIG. 4. Wave envelope over an infinite wedge-shaped region of randomness ($|Y|<X$) for medium nonlinearity $kA_0/\varepsilon=0.5$ and different roughness heights (a) $k\sigma/\varepsilon=0.5$ and (b) $k\sigma/\varepsilon=1.0$.

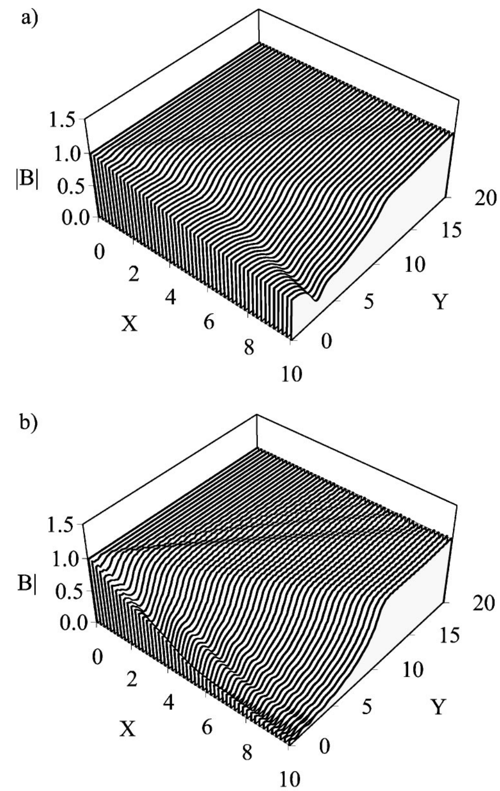

FIG. 5. Wave envelope over an infinite wedge-shaped region of randomness ($|Y|<X$) for strong nonlinearity $kA_0/\varepsilon=1.0$ and different roughness heights (a) $k\sigma/\varepsilon=0.5$ and (b) $k\sigma/\varepsilon=1.0$.

The case of a truncated wedge (a triangle) is even more interesting. For zero nonlinearity, there is a recovery of waves in the wake of the triangle ($X>5$) where there is again no disorder. An envelope depression (hole) is seen to form for higher roughness, while diffraction is strong outside $Y>X$ (Fig. 6). With moderate nonlinearity, attenuation is slowed, while recovery in the wake and formation of envelope holes are more evident (Fig. 7). For strong nonlinearity, these tendencies are very pronounced (Fig. 8) and six envelope holes are evident. Thus, delocalization is accompanied by hole formation.

We now give evidence that the envelope holes are essentially the analytical dark solitons represented by Eq. (53). First, in Table I, the computed slope of an envelope hole, c_{slope}, is compared with the theoretical slope $c_{|B|_{min}}$, calculated from Eq. (54) using the computed $|B_{min}|$, for the six observable holes. The discrepancies are about 2% or less, which can be attributed to the discreteness of data.

Second, corresponding to Fig. 8(b), where $kA_0/\varepsilon=k\sigma/\varepsilon=1$, we plot in Fig. 9 the local profiles of the six largest depressions at the stations $X=50,60,70,80,90,100$. For each depression, the computed profiles at all six stations fall on the same curve, which is indistinguishable from the theoretical profile of the same amplitude. This confirms that the depressions observed are dark solitons.

Thus, while inside the region of disorder randomness causes localization and nonlinearity causes delocalization, dark solitons emerge in the ordered wake by nonlinearity.

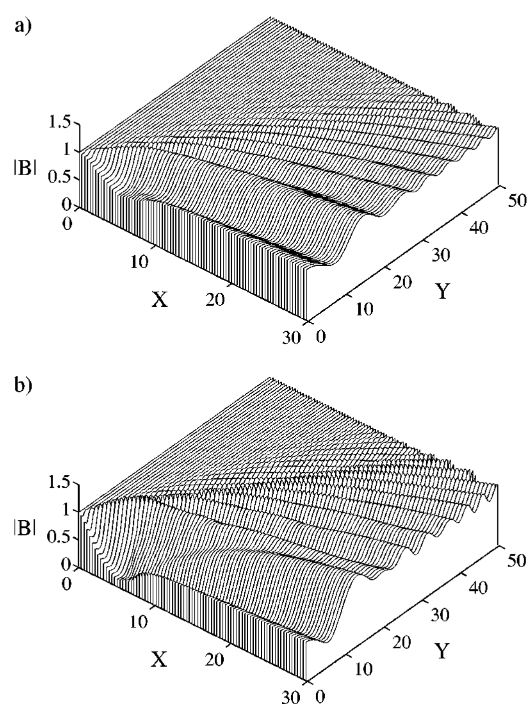

FIG. 6. Wave envelope over a triangular region of randomness ($0<X<5$, $|Y|<X$) for the linear limit $kA_0/\varepsilon=0.0$ and roughness heights (a) $k\sigma/\varepsilon=0.5$ and (b) $k\sigma/\varepsilon=1.0$.

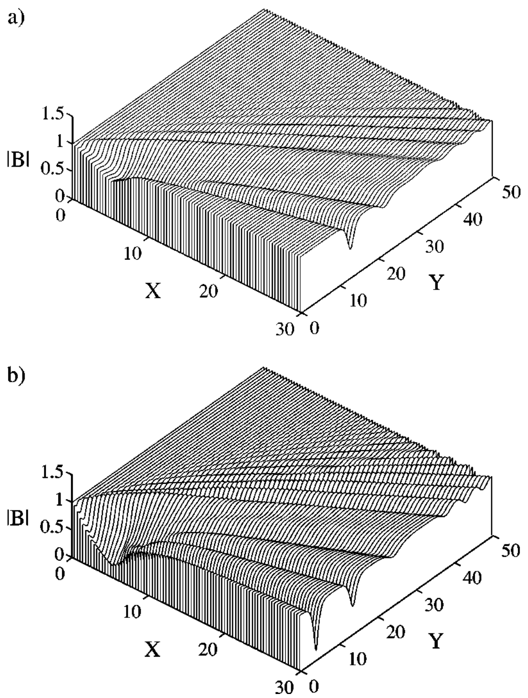

FIG. 7. Wave envelope over a triangular region of randomness ($0<X<5$, $|Y|<X$) for moderate nonlinearity $kA_0/\varepsilon=0.5$ and roughness heights (a) $k\sigma/\varepsilon=0.5$ and (b) $k\sigma/\varepsilon=1.0$.

This feature is reminiscent of the propagation of long waves from one constant depth, over a slope and onto another shallower and constant depth. Distortion over the slope is known to be followed by disintegration into several solitons, as

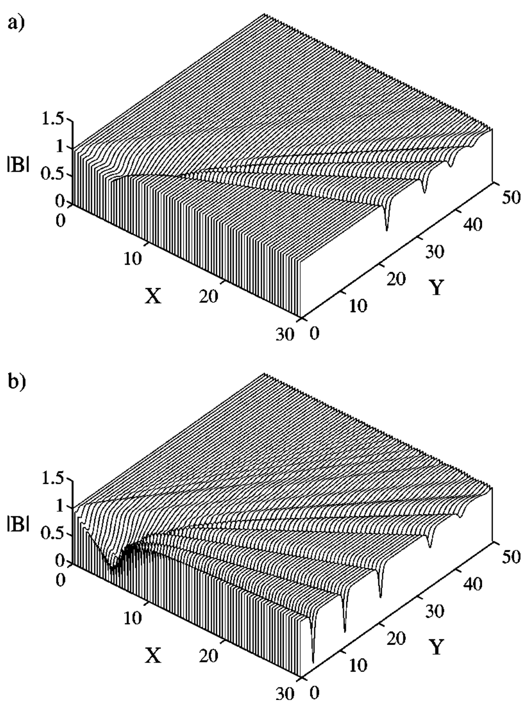

FIG. 8. Wave envelope over a triangular region of randomness ($0<X<5$, $|Y|<X$) for strong nonlinearity $kA_0/\varepsilon=1.0$ and roughness heights (a) $k\sigma/\varepsilon=0.5$ and (b) $k\sigma/\varepsilon=1.0$.

TABLE I. Inclinations of the dark solitons in Fig. 8(b). c_{slope} is the slope measured from the numerically computed envelope trough. $c_{|B|_{min}}$ is the theoretical slope based on the height of the computed envelope trough, $|B|_{min}$. $c_{least\ scatter}$ is the slope used to obtain the least scatter in Fig. 9.

Dark soliton number from x axis	c_{slope}	$\lvert B\rvert_{min}$	$c_{\lvert B\rvert_{min}}$	$c_{least\ scatter}$
1	0.1125	0.0629	0.1157	0.1141
2	0.4157	0.2300	0.4227	0.4175
3	0.7337	0.4045	0.7433	0.7325
4	1.2308	0.6785	1.2467	1.2275
5	1.5000	0.8356	1.5355	1.5100
6	1.7209	0.9425	1.7320	1.7200

shown by a theory of Korteweg-deVries type and by experiments [34].

VI. A QUARTER PLANE OF RANDOMNESS

Our final example is concerned with a quarter plane of disorder ($0<X<\infty$, $-\infty<Y<0$), which is representative of the corner of a large rectangular domain. The parameters are $kh=0.7$, $k/\alpha=3$ (hence $\beta^*\approx 1.654+1.618i$) and $kA_0/\varepsilon=k\sigma/\varepsilon=1$. As shown in Fig. 10, deep inside the zone of disorder (Y negative and large) the problem is one-dimensional in X and localization is exponential. For finite $Y>0$ and very large X, flattening of $|B|$ in Y across the transition is accompanied by a slow decay of $|B|$ in X, as expected from the parabolic nature of the Schrödinger equation (52).

VII. CONCLUDING REMARKS

In this paper we have treated two-dimensional wave diffraction and localization of weakly nonlinear surface water waves over a partly random bathymetry. The evolution equation is shown to be of the nonlinear Schrödinger form with a new linear term whose complex coefficient is deterministic

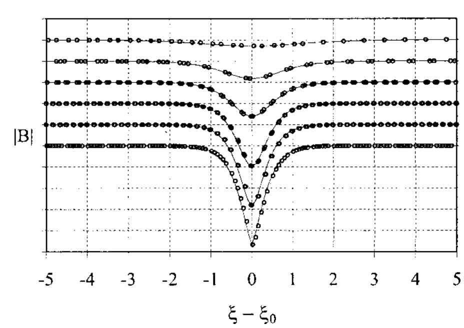

FIG. 9. Comparison of the six largest envelope holes found in Fig. 8(b) for $X=50,60,70,80,90,100$ with theoretical dark soliton envelopes. The variable on the abscissa is $\xi=Y-c_{least\ scatter}X$, where $c_{least\ scatter}$, listed in Table I, is the slope used to obtain the least scatter in the fit to the theoretical envelopes above. The unit on the ordinate is 0.2.

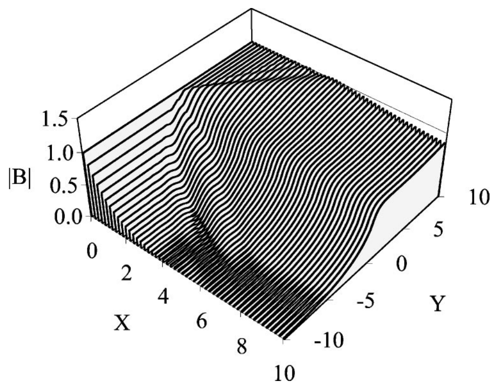

FIG. 10. Wave envelope over a quarter plane region of randomness $(0<X<\infty, \quad -\infty<Y<0)$ with $kA_0/\varepsilon = k\sigma/\varepsilon = 1.0$.

and depends on the statistical average of the random fluctuations [35]. While the disorder induces exponential attenuation in space, nonlinearity is seen to slow down the attenuation within, and to reduce the diffraction outside, the zone of disorder. If the random bathymetry has a finite area, dark solitons are created in the wake, similar to the fission of long solitons in shallow water governed by Boussinesq/KdV theories.

For oceanographic applications, an important task is to study random nonlinear waves of broad frequency band over a bathymetry with random fluctuations superposed on a gentle mean slope. The combination of geometrical optics, multiple scattering, and nonlinear diffraction should be a worthy challenge in wave dynamics.

Finally, the present method of homogenization, i.e., multiplescale expansions, appears to be very efficient to treat weak disorder, and can be extended to fully three-dimensional problems such as the scattering of sound by a dilute cloud of bubbles, treated by a diagrammatic theory by Ref. [36].

ACKNOWLEDGMENTS

We acknowledge with gratitude the financial support by US Army Corps of Engineers, Waterways Experiment Station, Vicksburg, Mississippi (Grant No. DACW 39-99-C-0033, Dr. Donald Resio), U.S. Office of Naval Research (Grant No. N00014-89J-3128, Dr. Thomas Swean), and U.S. National Science Foundation (Grant No. CTS-0075713, Dr. John Foss and Dr. C. F. Chen). J.H.P. also acknowledges the financial support of the Danish Technical Research Council (STVF Grant No. 990 3128).

APPENDIX: GREEN'S FUNCTION

Using polar coordinates and the Hankel transform, Green's function is formally found as

$$\begin{aligned}\mathcal{G} &= \frac{1}{2\pi}\int_0^\infty \frac{\kappa\cosh(\kappa z)+\dfrac{\omega^2}{g}\sinh(\kappa z)}{\dfrac{\omega^2}{g}\cosh(\kappa h)-\kappa\sinh(\kappa h)} J_0(\kappa|\vec{\xi}|)\,d\kappa \\ &= \frac{1}{4\pi}\int_0^\infty \frac{\kappa\cosh(\kappa z)+\dfrac{\omega^2}{g}\sinh(\kappa z)}{\dfrac{\omega^2}{g}\cosh(\kappa h)-\kappa\sinh(\kappa h)} H_0^{(1)}(\kappa|\vec{\xi}|)\,d\kappa \\ &\quad + \frac{1}{4\pi}\int_0^\infty \frac{\kappa\cosh(\kappa z)+\dfrac{\omega^2}{g}\sinh(\kappa z)}{\dfrac{\omega^2}{g}\cosh(\kappa h)-\kappa\sinh(\kappa h)} H_0^{(2)}(\kappa|\vec{\xi}|)\,d\kappa,\end{aligned} \tag{A1}$$

where $\vec{\xi}\equiv\vec{x}-\vec{x}'$ and $H_0^{(1)}$ and $H_0^{(2)}$ are Hankel functions of order zero of the first and second kinds, respectively.

In the complex plane of κ, the integrands have real poles at $\kappa=\pm k$, where k is the positive real root of the dispersion relation (12), and imaginary poles at $\pm ik_n$, where k_n are the positive real roots of

$$\omega^2 = gik_n\tanh(ik_nh) = -gk_n\tan(k_nh), \quad n=1,2,3,\ldots.$$

To ensure outgoing waves at infinity, the integration path along the positive real axis must be indented below the real pole at κ, for both integrals in Eq. (A1).

Note that as $r\to\infty$,

$$H_0^{(1)}(\kappa r)\sim\sqrt{\frac{2}{\pi\kappa r}}e^{i[\kappa r-(\pi/2)]},$$

$$H_0^{(2)}(\kappa r)\sim\sqrt{\frac{2}{\pi\kappa r}}e^{-i[\kappa r-(\pi/2)]}.$$

Thus, for the integral in Eq. (A1) involving $H_0^{(1)}$, we introduce a closed contour in the first quadrant by adding a circular arc of infinite radius and a vertical path C_+ circumventing all poles ik_n along the positive imaginary axis. For the integral in Eq. (A1) involving $H_0^{(2)}$, we introduce a closed contour in the fourth quadrant by adding a large circular arc and an indented vertical path C_- circumventing all poles $-ik_n$ along the negative imaginary axis. By standard application of the residue theorem, we evaluate the two contour integrals. The line integrals along the circular arcs vanish by Jordan's lemma. To the line integrals C_+ and C_-, the net contributions come from the infinitesimal semicircles around the imaginary poles and lead to an infinite series. The net contributions from the vertical segments between the semicircles vanish by pairwise cancellation from $C+$ and C_-. The result is Eq. (21).

[1] L. A. Chernov, *Wave Propagation in a Random Medium* (Dover, New York, 1967).
[2] A. Ishimaru, *Wave Propagation and Scattering in Random Media* (IEEE Press, New York, 1997).
[3] F. C. Karal and J. B. Keller, J. Math. Phys. **5**, 537 (1964).
[4] J. B. Keller, in *Proceedings of the 16th Symposium on Applied Mathematics* (American Mathematical Society, Providence, RI, 1964), p. 145.
[5] T. T. Soong, *Random Differential Equations in Science and Engineering* (Academic Press, New York, 1973).
[6] M. Asch, W. Kohler, G. C. Papanicolaou, M. Postel, and B. White, SIAM (Soc. Ind. Appl. Math.) Rev. **33**, 519 (1991).
[7] U. Frisch, in *Probabilistic Methods in Applied Mathematics*, edited by A. T. Bharucha-Reid (Academic Press, New York, 1968), Vol. 1, pp. 75–198.
[8] P. Sheng, *Scattering and Localization of Classical Waves in Random Media* (World Scientific, Singapore, 1990).
[9] P. Sheng, *Introduction to Wave Scattering, Localization, and Mesoscopic Phenomena* (Academic Press, San Diego, 1995).
[10] J. F. Elter and J. E. Molyneux, J. Fluid Mech. **53**, 1 (1972).
[11] P. Devillard, F. Dunlop, and B. Souillard, J. Fluid Mech. **186**, 521 (1988).
[12] A. Nachbin and G. C. Papanicolaou, J. Fluid Mech. **241**, 311 (1992).
[13] A. Nachbin, J. Fluid Mech. **296**, 353 (1995).
[14] P. A. Anderson, Phys. Rev. **109**, 1492 (1958).
[15] P. Devillard and B. Souillard, J. Stat. Phys. **43**, 423 (1986).
[16] B. Doucot and R. Rammal, Europhys. Lett. **3**, 969 (1987).
[17] R. Knapp, Physica D **85**, 496 (1995).
[18] J. C. Bronski, J. Stat. Phys. **92**, 995 (1998).
[19] J. Garnier, SIAM (Soc. Ind. Appl. Math.) J. Appl. Math. **58**, 1969 (1998).
[20] J. Garnier, Waves Random Media **11**, 149 (2001).
[21] S. A. Gredeskul and Y. S. Kivshar, Phys. Rep. **216**, 1 (1992).
[22] F. G. Bass, Y. S. Kivshar, V. V. Konotop, and Y. A. Sinitsyn, Phys. Rep. **157**, 63 (1988).
[23] J. Garnier, J. Stat. Phys. **105**, 789 (2001).
[24] C. C. Mei and J. H. Pihl, Proc. R. Soc. London, Ser. A **458**, 119 (2002).
[25] K. Hasselmann, Rev. Geophys. Space Phys. **4**, 1 (1966).
[26] R. B. Long, J. Geophys. Res. **78**, 7861 (1973).
[27] M. S. Howe, J. Fluid Mech. **45**, 785 (1971).
[28] R. R. Rosales and G. C. Papanicolaou, Stud. Appl. Math. **68**, 89 (1983).
[29] C. C. Mei and M. J. Hancock (unpublished).
[30] C. C. Mei, *Applied Dynamics of Ocean Surface Waves* (World Scientific, Singapore, 1989).
[31] We shall sometimes use the vector symbol $\vec{k}$ for compactness, although it only has the x component, i.e., $\vec{k}=(k,0)$.
[32] D. K.-P. Yue and C. C. Mei, J. Fluid Mech. **99**, 33 (1980).
[33] D. H. Peregrine, J. Aust. Math. Soc. B, Appl. Math. **25**, 16 (1983).
[34] O. S. Madsen and C. C. Mei, J. Fluid Mech. **39**, 781 (1969).
[35] Deductions from this deterministic theory represent the statistical average of many realizations, hence can only be checked by an ensemble of experiments.
[36] C. A. Condat and T. R. Kirkpatrick, in *Scattering and Localization of Classical Waves in Random Media* (World Scientific, Singapore, 1990), pp. 423–540.